TRAJECTORY TRACKING CONTROL OF A CART–PENDULUM SYSTEM USING BACKSTEPPING METHOD: SIMULATION AND EXPERIMENT

Hoang-Linh Le [1], Phong-Luu Nguyen [1], Duc-Thu Nguyen [2]*

[1] Ho Chi Minh City University of Technology and Engineering (HCM-UTE)
Vo Van Ngan Str., No. 01, Ho Chi Minh City (HCMC), Vietnam
[2] Ho Chi Minh City Power Corporation (EVNHCMPC)
Str. No 4, Di An ward, HCMC, Vietnam
* Corresponding author. E-mail: thund@hcmpc.com.vn

Abstract: This paper presents a nonlinear control strategy for trajectory tracking of a cart–pendulum system based on the backstepping approach. First, the nonlinear dynamic model of the system is formulated in a state-space representation. A systematic controller design procedure is then developed by introducing virtual control inputs. The stability of the closed-loop system is rigorously analyzed using Lyapunov theory, which guarantees the asymptotic convergence of the tracking errors. The proposed controller enables the cart position to accurately track a sinusoidal reference trajectory while maintaining the pendulum angle around the equilibrium point. Both simulation and experimental results demonstrate the effectiveness and stability of the proposed control method. The obtained results confirm that the controller provides satisfactory tracking performance for the nonlinear system.
Keywords: Backstepping control, Nonlinear control, Trajectory tracking, Inverted pendulum, Lyapunov stability.

1. Introduction

Inverted pendulum on a cart is a classical benchmark system in nonlinear control due to its nonlinear dynamics, inherent instability, and underactuated structure. Because of these characteristics, it has been widely used to evaluate advanced control algorithms and to validate theoretical control methods in both simulation and experimental studies. Control objective is typically to stabilize pendulum around upright equilibrium while regulating or tracking cart position.

Various control strategies have been proposed to address the control problem of inverted pendulum systems. Robust nonlinear control methods such as sliding mode control have been widely investigated due to their ability to handle disturbances and parameter uncertainties. For instance, backstepping sliding mode control has been applied to improve robustness for inverted pendulum systems under disturbances and uncertain parameters [2]. Other advanced approaches include adaptive neural network–based sliding mode control [3] and second-order sliding mode control combined with fuzzy adaptive techniques to enhance control performance and robustness [4]. In addition, hierarchical sliding mode control integrated with disturbance observers has been developed for trajectory tracking of wheeled inverted pendulum robots [5].

Among nonlinear control approaches, the backstepping method has attracted significant attention due to its recursive design procedure and strong stability guarantees based on Lyapunov theory. A robust adaptive backstepping controller for the inverted pendulum on a cart system was proposed in [1], demonstrating effective stabilization performance under model uncertainties. Furthermore, advanced backstepping-based control strategies such as command-filtered backstepping sliding mode control have been developed to improve the dynamic performance of rotary inverted pendulum systems [6].

Although many existing studies focus mainly on stabilizing the inverted pendulum around the equilibrium point, trajectory tracking control of the cart position remains a challenging problem because of nonlinear coupling dynamics and system instability. Therefore, developing an effective backstepping-based control strategy that ensures both pendulum stabilization and accurate trajectory tracking is still an important research topic.

In this paper, a backstepping control method is developed for trajectory tracking of an inverted pendulum on a cart system. The controller is designed based on Lyapunov stability theory to guarantee the stability of the closed-loop system while enabling the cart to track a desired reference trajectory. Simulation and experimental results are provided to demonstrate the effectiveness of the proposed control strategy.

2. Methodology

2.1. Inverted Pendulum on Cart Model

To investigate the effectiveness of the proposed control strategy, the inverted pendulum on a cart system is considered as the experimental platform. This system is widely used in control engineering as a classical benchmark for studying nonlinear, underactuated, and inherently unstable dynamics. The control objective is to maintain the pendulum in its upright equilibrium position while simultaneously controlling the motion of the cart along a desired trajectory. Due to its nonlinear characteristics and sensitivity to disturbances, the inverted pendulum system provides a suitable framework for evaluating the performance of advanced nonlinear control methods.

The physical configuration of the cart–pendulum system is illustrated in Fig. 1, where the pendulum can move between two equilibrium positions: the unstable upright position and the stable downward position. The upright configuration represents the main control challenge, as the system must continuously generate appropriate control inputs to keep the pendulum balanced while allowing the cart to move according to the reference trajectory.

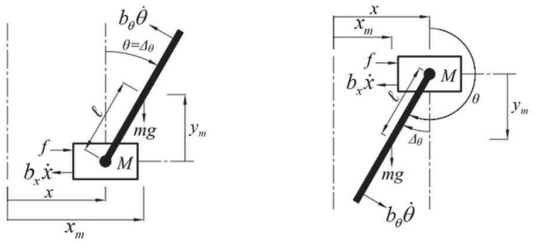


Fig. 1 Cart–pendulum system: upright equilibrium position (left) and downward hanging position (right).[7]

Tab. 1 The system parameter

No.	Symbol	Description	Value	Unit
1	m	Mass of the pendulum rod	0.084	kg
2	M	Mass of the cart	0.19008	kg
3	l	Length from pivot to pendulum center of mass	0.082	m
4	R	Radius of the drive pulley	0.00625	m
5	g	Gravitational acceleration	9.81	m/s^2
6	x	Cart position along the horizontal axis	n/a	m
7	θ	Pendulum angle with respect to the vertical axis	n/a	rad
8	u	Input voltage applied to the motor	n/a	V
9	$\dot{} = v_x$	Cart velocity	n/a	m/s
10	$\dot{\theta}$	Angular velocity of the pendulum	n/a	rad/s
11	b_x	Friction coefficient between cart and belt	1.4867	—
12	b_θ	Friction coefficient between pendulum and cart	1.3663×10^{-6}	—
13	B	Viscous friction coefficient of the motor shaft	5.8383×10^{-3}	—

Based on the Lagrange formulation, the nonlinear dynamic behavior of the system can be described by the following equations:

$$\begin{cases} \dfrac{d}{dt}\left(\dfrac{\partial L}{\partial \dot{x}}\right) - \dfrac{\partial L}{\partial x} = \tau_m \\ \dfrac{d}{dt}\left(\dfrac{\partial L}{\partial \dot{\theta}}\right) - \dfrac{\partial L}{\partial \theta} = 0 \end{cases} \quad (1)$$

where:

L = T- U : Lagrange operator

The differential equation form solved from (1) based on [7] is presented as follows:

$$M(q)\ddot{q} + V_M(q,\dot{q})\dot{q} + G(q) = \quad + w \quad (2)$$

where:

$q = [x \quad \theta]^T$ is the state vector representing the position and the pendulum angle.

$\dot{q} = [\dot{x} \quad \dot{\theta}]^T$ is the velocity vector representing the linear velocity of the cart and the angular velocity of the pendulum.

$\ddot{q} = [\ddot{x} \quad \ddot{\theta}]^T$is the acceleration vector of the generalized coordinates.

The matrices and vectors are defined as follows:

$M(q) = \begin{bmatrix} m+M & ml\cos\theta \\ ml\cos\theta & I+ml^2 \end{bmatrix}$: is the inertia matrix.

$V_m(q,\dot{q}) = \begin{bmatrix} 0 & -ml\dot{\theta}\sin\theta \\ 0 & 0 \end{bmatrix}$: is the Coriolis and viscous matrix.

$G(q) = \begin{bmatrix} 0 \\ -mgl\sin\theta \end{bmatrix}$: is the gravity vector.

$\tau = \begin{bmatrix} \tau_m \\ 0 \end{bmatrix}$: is the vector consisting of the motor torque and the control input.

$w = \begin{bmatrix} w_1 \\ w_2 \end{bmatrix}$: represents the friction force vector including the linkage friction components described in Tab. 1

The electromechanical dynamics of the motor can be expressed as

$$\tau = k_1 u - k_2\omega - k_3\tau_l \quad (3)$$

where $\tau$is the generated motor torque, $e$is the applied voltage, $\omega$is the motor angular velocity, and τ_l denotes the load torque.

The coefficients k_1, k_2, and $k_3$are defined as

$$k_1 = \frac{K_t}{R_m}, k_2 = \frac{K_t K_b}{R_m} + B, k_3 = \frac{J_m}{R_m}$$

where K_t is the motor torque constant, K_b is the back electromotive force (EMF) constant, $R_m$is the motor armature resistance, $B$is the viscous friction coefficient, and $J_m$is the rotor moment of inertia.

By substituting (3) and (2) into the system state equation, the dynamic model of the system can be expressed as

$$M(q)\ddot{q} + V_M(q,\dot{q})\dot{q} + G(q) = \begin{bmatrix} k_1 u \\ 0 \end{bmatrix} \quad (4)$$

where

$$M(q) = \begin{bmatrix} m+M+k_3 & \text{mlcos}(x_3) \\ \text{mlcos}(x_3) & I+ml^2 \end{bmatrix}$$

$$V_m = \begin{bmatrix} k_2 + b_1 + B - mlx_4^2\sin(x_3) \\ b_2 \end{bmatrix}$$

$$G = \begin{bmatrix} 0 \\ -mlg\sin(x_3) \end{bmatrix}$$

2.2. Backstepping controller

2.2.1. Backstepping controller design

The nonlinear state-space representation of the system can be written as

$$\begin{cases} \dot{x}_1 = x_2 \\ \dot{x}_2 = f_1(X) + g_1(X)u \\ \dot{x}_3 = x_4 \\ \dot{x}_4 = f_1(X) + g_1(X)u \end{cases} \quad (5)$$

Where: $X = [x_1, x_2, x_3, x_4]^T = [x, \dot{x}, \theta, \dot{\theta}]^T$: is the state vector. The functions $f_1(X)$, $f_2(X)$, $g_1(X)$, and $g_2(X)$ represent nonlinear system dynamics.

The control input is designed using the backstepping approach as:

$$\dot{x}_2 = U \quad (6)$$

Substituting this control input into (4.27), the error variable can be expressed as:

$$u = \frac{-f_1(X) + U}{g_1(X)} \quad (7)$$

Then, substituting the designed control signal into the second subsystem yields:

$$x_4 = f(X) + g(X)U \quad (8)$$

Where:

$$f(X) = f_2(X) - \frac{f_1(X)g_2(X)}{g_1(X)} \quad (9)$$

$$g(X) = \frac{g_2(X)}{g_1(X)} \quad (10)$$

By rearranging we obtain:

$$\begin{cases} \dot{x}_1 = \dot{q}_1 \\ \dot{x}_2 = \ddot{q}_1 = U \\ \dot{x}_3 = \dot{q}_2 \\ \dot{x}_4 = \ddot{q}_2 = f(X) + g(X)U \end{cases} \quad (11)$$

The control objective is to design a single control input u such that the system states $X = [x_1, x_2, x_3, x_4]^T$ track the desired states. For tracking control, the reference state vector is defined as : $X_d = [x_{1d}, x_{2d}, x_{3d}, x_{4d}]^T$.

The first virtual control variable of the system is defined as

$$z_1 = c_{11}r_1 + c_{12}r_2 + c_{13}\left(\dot{r}_2 - \dot{r}_1 g(X)\right) \quad (12)$$

Here, c_1, c_2, and $c_3$are design constants. The tracking errors are defined as $r_1 = x - x_d$ and $r_2 = \theta - \theta_d$, which represent the position and angular tracking errors, respectively.

Taking the time derivative of (12), we obtain

$$\dot{z}_1 = c_{11}\dot{r}_1 + c_{12}\dot{e}_{12} + c_{13}\left[\ddot{e}_{12} - \ddot{e}_{11}g(X) - \dot{e}_{11}\dot{g}(X)\right] \quad (13)$$

Substituting (11) into (13), we obtain

$$\dot{z}_1 = c_{11}\dot{r}_1 + c_{12}\dot{r}_2 + c_{13}\left[f(X) - \ddot{x}_{3d} + \ddot{x}_{1d}g(X) - \dot{r}_1\dot{g}(X)\right] \quad (14)$$

The stability function is defined as:

$$\alpha = -c_{12}\dot{r}_2 - c_{13}(f(X) - \ddot{x}_{3d} + g(X)\ddot{x}_{1d} - \dot{r}_1\dot{g}(X)) - k_{11}z_1 \quad (15)$$

The second virtual control variable of the system is defined as:

$$z_2 = c_{11}\dot{r}_1 - \alpha \quad (16)$$

Taking the time derivative of z_2, we obtain:

$$\dot{z}_2 = c_{11}(U - \ddot{x}_{1d}) + c_{12}\left(f(X) + g(X)U - \ddot{x}_{3d}\right) + c_{13}\begin{pmatrix} \dot{f}(X) - \dddot{x}_{3d} + \dddot{x}_{1d}g(X) + \dot{g}(X)\ddot{x}_{1d} \\ -\ddot{g}(X)(\dot{x}_1 - \dot{x}_{1d}) - \dot{g}(X)(U - \ddot{x}_{1d}) \end{pmatrix} + k_{11}\dot{z}_1 \quad (17)$$

The desired dynamics oare given as follows::

$$\dot{z}_2 = -z_1 - k_{12}z_2 \quad (18)$$

In which: k_{12} is design constants.

$$U = \frac{\begin{array}{l} c_{11}\ddot{x}_{1d} + c_{12}\ddot{x}_{3d} - c_{13}f(X) + c_{13}\dddot{q}_{2d} + c_{13}(\dot{x}_1 - \dot{x}_{1d})f(X) \\ - c_{13}\dot{g}(X)\ddot{x}_{1d} - k_1\dot{z}_1 - z_1 - k_{12}z_2 \end{array}}{c_{11} + c_{12}g(X) - c_{13}g(X) - c_{13}g_{13}(\dot{x}_1 - \dot{x}_{1d}) - c_{13}\dot{g}f(X)} \quad (19)$$

2.2.2. Stability analysis

The Lyapunov function is selected as

$$V = \frac{1}{2}z_1^2 + \frac{1}{2}z_2^2 \quad (20)$$

Taking the time derivative of Vyields

$$\dot{V} = z_1\dot{z}_1 + z_2\dot{z}_2 \quad (21)$$

Substituting (18) and (13) into the above equation gives:

$$\dot{V} = -k_1z_1^2 - k_2z_2^2 \quad (22)$$

Since $k_{11} > 0$ and $k_{12} > 0$, it follows that $\dot{V} \le 0$.

Rearranging the above equation gives

$$\int_0^t \left(k_{11}z_1^2 + k_{12}z_2^2\right)d\tau = V(0) - V(t). \quad (23)$$

Since $V(t) \ge 0$, we have

$$\int_0^t \left(k_{11}z_1^2 + k_{12}z_2^2\right)d\tau \le V(0). \quad (24)$$

Therefore, $z_1 \in L_2, z_2 \in L_2$.

Since z_1 and z_2 are bounded, and the closed-loop auxiliary error dynamics are given by

$$\dot{z}_1 = -k_{11}z_1 + z_2, \dot{z}_2 = -z_1 - k_{12}z_2, \quad (25)$$

it can be concluded that $\dot{z}_1$ and $\dot{z}_2$ are also bounded. Hence, z_1 and z_2 are uniformly continuous. According to Barbalat's lemma, if a function is uniformly continuous and its squared integral is finite, then the function converges to zero as time approaches infinity.

3. Simulation results

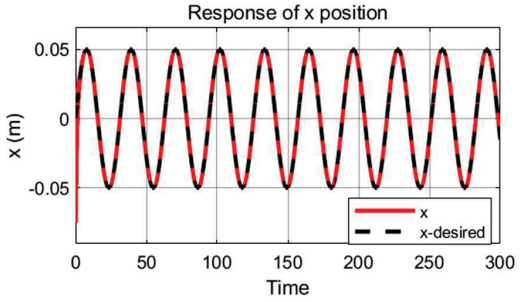


Fig. 2 Position response x tracking a sinusoidal reference trajectory.

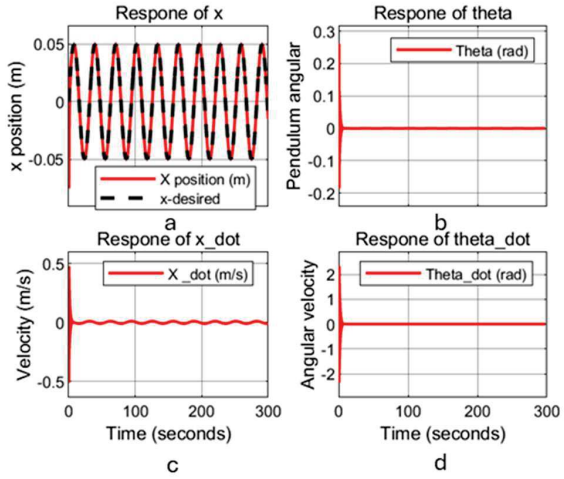


Fig. 3 (a) Position tracking response x for a sinusoidal reference trajectory, (b) Angular response of the pendulum θ, (c) Velocity response of the cart $\dot{x}$., (d) Angular velocity response of the pendulum $\dot{\theta}$.

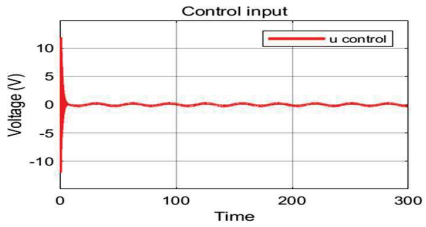


Fig. 4 Control input signal u

The simulation results presented in Fig. 2, Fig. 3(a–d), and Fig. 4 demonstrate the effectiveness and stability of the proposed backstepping controller in achieving trajectory tracking for the inverted pendulum on a cart system. As illustrated in Fig. 2, the cart position closely follows the desired reference trajectory $_{desired}$after a short transient period. The tracking performance shows that the actual trajectory converges rapidly to the reference signal with negligible steady-state error, indicating the good tracking capability of the designed controller. The periodic reference signal is reproduced accurately by the system response, confirming the robustness of the control strategy under dynamic conditions.

More detailed system responses are depicted in Fig. 3(a–d). In Fig. 3(a), the cart position response further confirms that the system output remains bounded and maintains close agreement with the desired trajectory throughout the simulation time. Fig. 3(b) shows the response of the pendulum angle θ, which is maintained around the upright equilibrium position (approximately 0rad). This result indicates that the proposed control law successfully stabilizes the inherently unstable pendulum while simultaneously allowing the cart to track the desired motion trajectory. Additionally, the velocity responses shown in Fig. 3(c) and Fig. 3(d) illustrate that both the cart velocity $\dot{x}$and the angular velocity $\dot{\theta}$converge quickly after the initial transient phase and remain bounded with small oscillations. These responses reflect the good dynamic characteristics and stability of the closed-loop system under the designed backstepping control scheme.

The control input signal presented in Fig. 4 shows an initially large control effort at the beginning of the simulation, which is necessary to rapidly stabilize the pendulum and drive the system states toward the desired operating conditions. After the transient phase, the control signal gradually settles into a bounded oscillatory behavior with relatively small amplitude, corresponding to the periodic reference trajectory of the cart. This indicates that the controller is capable of maintaining stable trajectory tracking while keeping the control effort within a reasonable range.

Overall, the simulation results confirm that the proposed backstepping-based control strategy ensures stable system behavior, accurate trajectory tracking, and effective stabilization of the inverted pendulum. The obtained responses demonstrate that the controller provides fast convergence, bounded system states, and acceptable control effort, highlighting its suitability for implementation in practical inverted pendulum systems.

2.1. Experimental results

The experimental setup used in this study is shown in Fig. 5, similar to the configuration presented in [8]. The system consists of a cart–pendulum mechanism mounted on a linear rail, where the cart is actuated to move along the horizontal direction. A rigid pendulum is attached to the cart through a rotational joint, allowing it to swing freely in the vertical plane. Sensors are employed to measure the cart position and the pendulum angle, which are used as feedback signals for the control algorithm. This experimental platform provides a practical environment to evaluate the effectiveness of the proposed control strategy in stabilizing the pendulum and achieving trajectory tracking of the cart under real operating conditions.

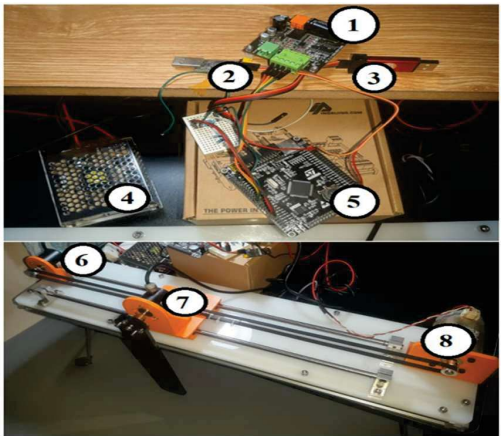


Fig. 5 Experimental setup and model

The experimental platform is composed of several hardware components, including:

1. An MKS H3615NS H-bridge motor driver used to control the motor actuation.
2. A CH340G USB-to-TTL converter module for serial communication between the controller and the computer.
3. An ST-LINK V2 programmer/debugger for programming and debugging the STM32 microcontroller.
4. A power supply module converting 220 VAC to 24 VDC to provide the required operating voltage for the system.
5. An STM32F407VET6 development board serving as the main controller for implementing the control algorithm.
6. An incremental encoder with 2500 pulses for measuring the cart position.
7. Another 2500-pulse incremental encoder used to measure the pendulum angle.
8. A NF5475 servo motor that drives the cart along the linear track.

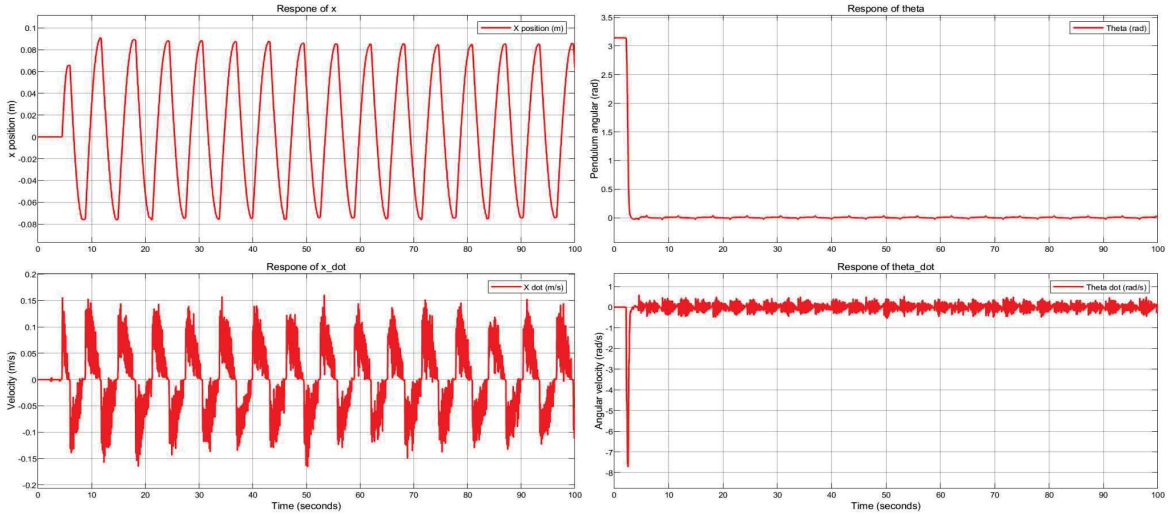


Fig. 6 Experimental responses of the system: (a) position tracking response $x$for a sinusoidal reference trajectory, (b) angular response of the pendulum θ, (c) velocity response of the cart $\dot{x}$, and (d) angular velocity response of the pendulum $\dot{\theta}$.

The experimental responses of the cart--pendulum system are presented in Fig. 7. As shown in Fig. 7(a), the cart position (x) follows a sinusoidal trajectory with bounded oscillations after the initial transient period. The measured cart displacement varies approximately within the range of (-0.08) m to (0.09) m, which is consistent with the imposed periodic motion. Although small deviations and waveform distortions appear in the experimental response, the cart position remains stable and repeats the desired oscillatory behavior throughout the test.

Fig. 7(b) shows the pendulum angular response (θ). At the beginning of the experiment, the pendulum angle starts from a large initial deviation of about (3.1) rad. Under the action of the proposed backstepping controller, the pendulum is rapidly driven toward the upright equilibrium position. The settling process occurs within approximately (4)-(5) s, after which the angle remains close to (0) rad with only small residual oscillations. This result verifies the stabilizing capability of the proposed controller under real experimental conditions.

The velocity responses are shown in Fig. 7(c) and Fig. 7(d). The cart velocity ($\dot{x}$) exhibits a periodic behavior corresponding to the sinusoidal cart motion, with its magnitude mainly bounded within approximately ($\pm$ 0.15) m/s. Meanwhile, the pendulum angular velocity ($\dot{\theta}$) presents a large initial peak during the stabilization phase, then quickly decreases and remains bounded around the equilibrium region. The high-frequency fluctuations observed in both velocity signals are mainly caused by encoder quantization, measurement noise, friction, actuator dynamics, and unmodeled disturbances in the experimental setup.

The experimental results confirm that the proposed backstepping controller can stabilize the pendulum near the upright equilibrium position while maintaining bounded cart trajectory tracking. Compared with the simulation results, the experimental responses contain larger noise and small tracking deviations due to practical limitations of the hardware system. Nevertheless, all system states remain bounded, and the pendulum angle converges to a small neighborhood around zero. Therefore, the experimental results demonstrate the practical feasibility and robustness of the proposed control method.

5. Conclusions

This paper presented a nonlinear control strategy based on the backstepping approach for trajectory tracking of the considered system. The nonlinear dynamic model was first formulated in a state-space representation, and a systematic controller design procedure was developed using virtual control inputs. The stability of the closed-loop system was rigorously analyzed using Lyapunov theory, ensuring that all tracking errors converge asymptotically to zero.

Simulation and experimental results demonstrated that the proposed controller achieves accurate trajectory tracking for the cart position while maintaining the pendulum angle around the equilibrium point. The responses of the system states, including position, velocity, angle, and angular velocity, confirmed the effectiveness and stability of the control scheme under sinusoidal reference trajectories.

The obtained results verify that the proposed control method provides satisfactory tracking performance and robustness for the nonlinear system. Future work will focus on improving the controller performance under external disturbances and parameter uncertainties, as well as extending the approach to more complex nonlinear systems.

Acknowledgement

This research was funded by Ho Chi Minh City University of Technology and Engineering (HCM-UTE), Vietnam, under grant No. SV2026-236. We want to give thanks to PhD. Van-Dong-Hai Nguyen (HCM-UTE) due to his supervision. We, authors, are grateful to those supports. Link video of system's operation is: https://www.youtube.com/watch?v=cwG7xhNV7dg&feature=youtu.be

6. References

[1] Rudra S., Barai R.K.: "Robust Adaptive Backstepping Control of Inverted Pendulum on Cart System", International Journal of Control and Automation, Vol. 5, No. 1, pp. 13-26, 2012.

[2] Ma'arif A., Heryanto M.A., Susanto E., Pramudita B.A.: "Backstepping Sliding Mode Control for Inverted Pendulum System with Disturbance and Parameter Uncertainty", Journal of Robotics and Control, Vol. 3, No. 1, pp. 86-92, 2021.

[3] Gupta N., Dewan L.: "Adaptive Neural Network-Based Sliding Mode Control of Rotary Inverted Pendulum System", Journal of Control and Decision, 2024.

[4] Leng X.: "Second-Order Sliding Mode Optimization Control of Inverted Pendulum System Based on Fuzzy Adaptive Technology", Frontiers in Mechanical Engineering, Vol. 10, Article 1458852, 2024.

[5] Hou M., Zhang Z., Li J., Wang X.: "Hierarchical Sliding Mode Control Combined with Nonlinear Disturbance Observer for Wheeled Inverted Pendulum Robot Trajectory Tracking", Applied Sciences, Vol. 13, No. 7, Article 4350, 2023.

[6] Mofid O., Rahmani A., Ghanbari M: "Adaptive Finite-Time Command-Filtered Backstepping Sliding Mode Control for Stabilization of a Disturbed Rotary-Inverted-Pendulum with Experimental Validation", Journal of Vibration and Control, Vol. 29, No. 5-6, pp. 1431-1446, 2023.

[7] Saco R.: "Subspace Identification of an Inverted Pendulum on a Cart using State Variables Transformation," IFAC-PapersOnLine, vol. 52, no. 11, pp. 244-249, 2019.

[8] Hoang D.-P.: "A Survey of Experimental LQR for Cart and Pole ", *J Fuzzy Syst Control*, vol. 2, no. 2, pp. 97–103, May 2024.